However, it is possible that hydrogen bonding between the solvent molecules H_2O and the nitrogen atoms of the CN ligands is effective. This bonding reduces the density of the π-electrons in the neighborhood of the central ion, and the overlap becomes weaker. Thus, the energy gap between the HOMO and the LUMO is enlarged. With increasing pressure, this effect will be strengthened, and as a consequence, absorption bands II–V are shifted to higher energies. That bands III and V show distinctly larger blue shifts than band II can be traced back to the different symmetries of the MO's from which the corresponding excitations start. Whereas the HOMO of bands III and V, $e_g(5d_{xy}, d_{yz}, \pi)$, contains a π-component due to the metal–ligand overlap, the HOMO of band II, $a_{1g}(5d_{z^2})$, is a pure metal state. This speculative model is supported by the above-mentioned dependence of the absorption energies on the solvent, where, with increasing protic character of the solvent, bands II–V are blue shifted.

Acknowledgment. This research has been supported by the Deutsche Forschungsgemeinschaft and the Fonds der Chemischen Industrie.

Metallacarboranes in Catalysis. 8. I: Catalytic Hydrogenolysis of Alkenyl Acetates. II: Catalytic Alkene Isomerization and Hydrogenation Revisited

James A. Belmont, Jorge Soto, Roswell E. King, III, Andrew J. Donaldson, John D. Hewes, and M. Frederick Hawthorne*

Contribution from the Department of Chemistry and Biochemistry, The University of California at Los Angeles, Los Angeles, California 90024. *Received October 31, 1988*

Abstract: Part I of this study describes the facile hydrogenolysis (and deuteriolysis) of alkenyl acetates, such as isopropenyl acetate (D) and 1-phenylvinyl acetate (E), with rhodacarborane catalyst precursors to yield acetic acid and the corresponding alkene. The catalyst precursors employed were [*closo*-3,3-$(PPh_3)_2$-3-H-3,1,2-$RhC_2B_9H_{11}$] (I), [*closo*-2,2-$(PPh_3)_2$-2-H-2,1,7-$RhC_2B_9H_{11}$] (II), and [*closo*-2,2-$(PPh_3)_2$-2-H-2,1,12-$RhC_2B_9H_{11}$] (III). The hydrogenolysis of alkenyl acetates D and E produced propene and styrene, respectively, along with acetic acid in essentially quantitative yields. Deuterium at Rh was demonstrated not to enter the hydrogenolysis reaction. Use of D_2 as the reducing agent with I and E resulted in the incorporation of deuterium into reactant E and products. Styrene produced in these reactions was predominantly d_1 with appreciable quantities of d_0 and d_2. Ethylbenzene, a byproduct resulting from the hydrogenation of styrene, contained only traces of d_0 species and was largely d_1, d_2, and d_3. The acetic acid formed in these reactions was isotopically pure CH_3COOD. The rate law for E hydrogenolysis with I contained no term showing hydrogen dependence. These results suggest a reaction mechanism for hydrogenolysis that is based upon the relatively slow formation and decomposition of a very reactive rhodium(III) monohydride formed through the regioselective oxidative addition of Rh^I (in the exo-nido tautomer of the rhodacarborane) to terminal B–H bonds. The monohydride produced in this fashion then enters a cyclic heterolysis process with H_2 which leads to rapid product formation. This mechanism suggests that slow B–D/C–H exchange should occur between I-d_9 (B–D at all vertices of I) and an isotopically normal alkane, such as 1-hexene (B), during alkene isomerization. Such exchange was observed and shown to be regioselective. This new information predicated part II of this study, which is devoted to a modification of previously advanced proposals for the mechanisms of alkene isomerization and hydrogenation with rhodacarborane precursors. The facile and regioselective exchange of B–H in [*exo-nido*-$(PPh_3)_2$Rh-μ-7,8-$(CH_2)_3$-7,8-$C_2B_9H_{11}$] (IV) with D_2 was examined and shown to be electrophilic in character and to apparently proceed through very reactive monohydride intermediates. These new data coupled with previously reported results allow the formulation of unified mechanisms for B–H/D_2 and B–H/C–D exchange, alkenyl acetate hydrogenolysis, alkene isomerization, and alkene hydrogenation based upon the key B–Rh^{III}–H species formed by the regioselective oxidative addition of terminal B–H bonds to Rh^I centers. Thus, the effective catalytic sites in all of these reactions appear to be an array of B–Rh^{III}–H centers formed reversibly from the Rh^I present in *exo-nido*-rhodacarborane tautomers which are, in turn, in equilibrium with their corresponding closo tautomers. In deuterium-labeling reactions, the marked difference in regiospecificity displayed by I in contrast to the sterically encumbered IV is shown to be in agreement with these new proposals.

The insertion of alkenes into metal hydride linkages and the microscopic reverse of this reaction (β-elimination) are ubiquitous throughout organometallic chemistry.[1] However, a variant of this set of reactions in which the alkene is an alkenyl acetate presents the possibility of observing another sort of β-elimination from the metal β-acetatoalkyl formed by insertion.[2] This reaction course results in the formation of metal acetate and the alkene derived from the alkenyl acetate by formal interchange of the acetate group with hydride. The actual fate of alkenyl acetates in the presence of metal hydrides has generally been determined by the number of available hydride ligands attached to the metal center. Thus, monohydrides provide stoichiometric cleavage of alkenyl acetate to metal acetate and alkene[2] (Scheme I), while dihydrides such as $H_2RhCl(PPh_3)_2$ can provide alkyl acetates via

Scheme I

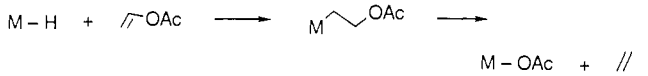

Scheme II

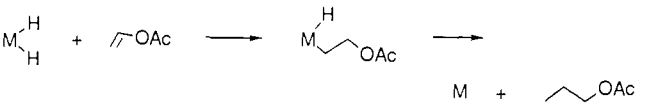

(1) Collman, J. P.; Hegedus, L. S.; Norton, J. R.; Finke, R. G. *Principles and Applications of Organotransition Metal Chemistry*; University of Science Books: Mill Valley, CA, 1987.

(2) (a) Abatjoglow, A. G.; Bryant, D. R.; D'Esposito, L. C. *J. Mol. Catal.* **1983**, *18*, 381. (b) Komiya, J.; Yamamoto, A. *J. Organomet. Chem.* **1975**, *87*, 333.

0002-7863/89/1511-7475$01.50/0

Scheme III

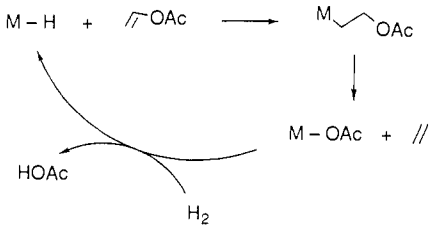

catalytic alkenyl acetate hydrogenation[3] (Scheme II). In the latter case, transfer of the second hydride to carbon with reductive elimination of alkyl acetate is favored over hydridometal acetate and alkene formation under normal hydrogenation conditions. We have confirmed that dihydride precursors such as $[(PPh_3)_3RhCl]$ and $[(COD)Rh(PPh_3)_2]^+$ produce clean catalytic hydrogenation of alkenyl acetates.

In part I of this two-part paper, we report the discovery of the facile catalytic hydrogenolysis of alkenyl acetates using *closo*-bis(triphenylphosphine)hydridorhodacarboranes as catalyst precursors near room temperature and with less than 1 atm of H_2 partial pressure. These new reactions are shown to proceed in accord with Scheme III and to result from a previously unrecognized set of equilibria associated with the rhodacarborane catalyst precursors described elsewhere[4,5] in conjunction with alkene hydrogenation, isomerization, and related reactions. Many of the unusual characteristics of this family of catalysts were previously ascribed[4,5] to the expected poor electron-donating ability of B–H bonds when serving as ligands to Rh in chelated exo-nido intermediates containing the $[\eta^2$-*nido*-$C_2B_9H_{12}]^-$ family of terminal BH two-electron donors. In view of the results reported here, the earlier mechanistic explanations of alkene hydrogenation and isomerization brought about through rhodacarborane catalysis are, in part, incorrect. However, when these older data are coupled with recently obtained experimental results, a set of unified and novel reaction mechanisms emerge. These new propositions will be developed as the present two-part study unfolds.

I. Hydrogenolysis of Alkenyl Acetates

The initial study reported here describes the catalytic hydrogenolysis of isopropenyl acetate (D) using the catalytic precursors[6] [*closo*-3,3-$(PPh_3)_2$-3-H-3,1,2-$RhC_2B_9H_{11}$] (I), [*closo*-2,2-$(PPh_3)_2$-2-H-2,1,7-$RhC_2B_9H_{11}$] (II), and [*closo*-2,2-$(PPh_3)_2$-2-H-2,1,12-$RhC_2B_9H_{11}$] (III). In addition, a kinetic study of the hydrogenolysis of 1-phenylvinyl acetate (E) was carried out using I as the catalyst source. These studies, when combined with related deuterium-scrambling experiments, have enhanced our understanding of the mechanisms of not only alkenyl acetate hydrogenolysis but previously reported[4,5] alkene isomerization and alkene and acrylate ester hydrogenation reactions, which are treated in the second part of this report.

Results and Discussion

In the absence of H_2, D reacts with I in tetrahydrofuran (THF) solution at 40 °C to slowly produce propene and the acetate species [*closo*-3,3-$(PPh_3)_2$-3-$OCOCH_3$-3,1,2-$RhC_2B_9H_{11}$] and [*closo*-3-PPh_3-3,3-η^2-$OCOCH_3$-3,1,2-$RhC_2B_9H_{11}$]. At 80 °C in benzene solution, these same reactants produce a bis(triphenylphosphine) complex which is orthometalated. These stoichiometric reactions are fully described elsewhere.[7] However, since the two rhodium acetate species mentioned above rapidly react with H_2 in the presence of added PPh_3 to produce acetic acid and I, it follows that acetate formation coupled with the H_2 reaction constitutes a closed system for the hydrogenolysis of D albeit in two distinct groups of reactions which apparently proceed through the agency of closo intermediates. This is not the same reaction sequence responsible for the catalytic hydrogenolysis of D with precursor I, which is of interest here, since it will be shown that the hydride ligand of the $HRh^{III}L_2$ vertex of I is not involved in direct D hydrogenolysis.

Table I. Hydrogenolysis of 0.20 M Isopropenyl Acetate (D) in THF at 40.8 °C Using 9.9×10^{-4} M H_2 and Rhodacarborane Catalyst Precursors

catalyst precursor	$[Rh]_t$[a]	mol equiv H_2 consumed	mol equiv CH_3COOH produced[b]
I	4.9×10^{-3}	1.70[c]	0.96
II	1.6×10^{-2}	1.70[c]	0.95
III	1.1×10^{-2}	1.77[d]	0.94
e	3.7×10^{-3}	1.00	0.00
f	8.9×10^{-3}	1.00	0.00

[a] Total Rh, M. [b] Determinated by GLC or by titration with standard base. [c] Sharp decrease in rate of H_2 uptake observed near 1.00 mol equiv of H_2 consumed. [d] No abrupt change observed in rate of H_2 uptake near 1.0 mol equiv of H_2 consumed. [e] $(PPh_3)_3RhCl$ as catalyst in the presence of 3.7×10^{-3} M PPh_3. [f] $[(COD)Rh(PPh_3)_2]^+PF_6^-$ employed as catalyst precursor.

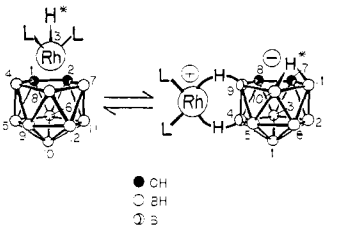

Figure 1. Representation of closo/exo-nido equilibrium showing the regiospecific transfer of H* between *closo*-I and one isomer of *exo-nido*-I. The vertices of the closo and exo-nido tautomers are numbered using the closo and nido numbering conventions, respectively.

Hydrogenolysis of Isopropenyl Acetate (D). Table I summarizes representative data for the hydrogenolysis of D using catalyst precursors I–III in the absence of added PPh_3 and the results of hydrogenation experiments with $[(PPh_3)_3RhCl]$ and $[(COD)Rh(PPh_3)_2]^+PF_6^-$ as catalyst precursors. The latter two catalyst systems produced isopropyl acetate exclusively, while the rhodacarborane systems gave nearly 1 mol equiv each of acetic acid and propene (identified by MS and ^1H FT NMR). Following the consumption of 1 mol equiv of H_2, an abrupt change was observed in the rate of H_2 consumption and the propene product was slowly hydrogenated. This rate behavior was unsatisfactory with respect to possible kinetic studies since the hydrogenolysis of D could not be cleanly separated from the propene hydrogenation. Nonetheless, it was shown that the addition of 4.0 mol equiv of $Cs^+[nido$-7,8-$C_2B_9H_{12}]^-$ per mole of I to a D hydrogenolysis reaction did not depress the rate of reaction when compared to an identical experiment carried out in the absence of added carborane ligand. Thus, $[(PPh_3)_2Rh(THF)_2]^+$ was ruled out as an active catalyst produced via closo-exo-nido tautomerization[4] of I followed by reversible dissociation of this cation from the exo-nido isomer. As mentioned above, this point was checked independently by virtue of the fact that $[(COD)Rh(PPh_3)_2]^+$ did not produce hydrogenolysis products when employed as the catalyst precursor in THF solution.

As in our earlier studies[4] with the closo catalyst precursor I, this hydridorhodacarborane was labeled with deuterium at the Rh vertex, giving I-3-d_1 with 95% isotopic purity (^1H FT NMR estimation) and the labeled precursor employed in an otherwise normal hydrogenolysis experiment. The samples of I recovered from this experiment after 9 and 25 turnovers of Rh showed 89% and 88%, respectively, of the D label remaining. As in previously reported cases,[4] these results prove that *closo*-I is not directly involved in the hydrogenolysis step but that intermediates derived

(3) Candlin, J. P.; Oldham, A. R. *Discuss. Faraday Soc.* **1968**, *46*, 60.
(4) Behnken, P. E.; Belmont, J. A.; Busby, D. C.; Delany, M. S.; King, R. E.; Kreimendahl, C. W.; Marder, T. B.; Wilczynski, J. J.; Hawthorne, M. F. *J. Am. Chem. Soc.* **1984**, *106*, 3011.
(5) Behnken, P. E.; Busby, D. C.; Delaney, M. S.; King, R. E.; Kreimendahl, C. W.; Marder, T. B.; Wilczynski, J. J.; Hawthorne, M. F. *J. Am. Chem. Soc.* **1984**, *106*, 7444.
(6) Baker, R. T.; Delaney, M. S.; King, R. E.; Knobler, C. B.; Long, J. A.; Marder, T. B.; Paxson, T. E.; Teller, R. G.; Hawthorne, M. F. *J. Am. Chem. Soc.* **1984**, *106*, 2965.
(7) King, R. E.; Busby, D. C.; Hawthorne, M. F. *J. Organomet. Chem.* **1985**, *279*, 103.

Table II. Collected Rate Data for the Hydrogenolysis of 1-Phenylvinyl Acetate (E) in THF at 40.8 °C Using I as the Catalyst Precursor

$10^2[Rh]_t$	$10^3[PPh_3]$	$10^3[H_2]$	$10[(E)]_0$	10^5k_{obs}, s^{-1}	10^6k_h, s^{-1}
0.52	4.48	1.02	2.59	0.290	2.49
2.14	4.44	1.02	2.59	1.07	2.22
3.19	4.44	1.02	2.59	1.57	2.18
2.14	1.53	1.02	2.59	2.24	1.60
2.14	2.16	1.02	2.59	2.07	2.08
2.14	9.16	1.02	2.59	0.407	1.74
2.14	4.44	0.273	2.59	0.936	1.94
2.14	4.44	0.438	2.59	0.982	2.03
2.14	4.44	1.98	2.59	1.04	2.16
2.14	4.44	1.02	0.65	0.921	1.91
2.14	4.44	1.01	1.29	1.11	2.30
2.14	4.44	1.02	1.90	0.985	2.04
2.14	4.48	1.02	3.37	1.05	2.19
2.14	4.48	1.02	2.56[a]	0.00	0.00

[a] Concentration of 1-phenylethyl acetate.

from the exo-nido tautomer of I are responsible for catalysis. This conclusion is based upon the demonstration[8] that the hydride ligand of the $HRh^{III}L_2$ vertex present in *closo*-I is reversibly and regiospecifically transferred to the B–H–B bridge present in each member of the set of mutually interconverting isomers of *exo-nido*-I. Consequently, the Rh^I centers present in the *exo-nido*-I tautomers may initiate reactions leading to catalysis, while the deuterium originally present in *closo*-I-*3*-d_1 is excluded from participation in this reaction[4] (Figure 1).

Having demonstrated that the catalytic hydrogenolysis of D is in apparent agreement with the simplified Scheme III using exo-nido-derived intermediates available from I–III, it was important to establish the rate law for a representative hydrogenolysis reaction and to compare the result with that observed[4] in simple alkene hydrogenation. The determination of the extent of deuterium incorporation in both reactants and products as a function of time was also required to assess the importance of β-hydride elimination from alkyl intermediates. With these desired studies in mind, 1-phenylvinyl acetate (E) was selected as a substrate due to its inability to isomerize, as well as the low vapor pressures of the acetate and its hydrogenolysis product, styrene. Furthermore, styrene is hydrogenated to ethylbenzene much more slowly than E is hydrogenolyzed. Hydrogenation of E was not observed with precursor I (limit of detection of 1-phenylethyl acetate, 0.2% conversion).

Kinetics of 1-Phenylvinyl Acetate Hydrogenolysis Using Catalyst Precursor I. In previously reported studies of rhodacarborane reactions with unsaturated esters, chelated adducts derived from *closo*-hydridorhodacarboranes such as I were observed with *n*-butyl acrylate,[5] while II was shown to form two diastereomerically related chelate adducts with vinyl acetate.[7] Prior to undertaking kinetic measurements that utilized E and I, it was established by variable-temperature $^{31}P\{^1H\}$ FT NMR experiments that E and I did not produce detectable concentrations of chelated adducts at the temperature chosen for kinetic studies, 40.8 °C.

The rate of E hydrogenolysis with I was monitored at constant H_2 pressure with an automatic hydrogen titrator[4,9] in THF solution at 40.8 °C. Added PPh_3 was present in each rate run. Variation of the initial concentrations of I, PPh_3, and H_2, all of which were unchanged throughout each experiment as E was consumed, produced the rate law shown in eq 1. Most interesting was the

$$\frac{-d[H_2]}{dt} = k_{obs}[E] = \frac{k_h[Rh]_t[E]}{[PPh_3]} \quad (1)$$

fact that eq 1 prevailed at all H_2 pressures investigated ($(0.273–1.98) \times 10^{-3}$ M H_2), and consequently *the hydrogenolysis reaction was independent of* $[H_2]$ *within the concentration range investigated.* Table II presents the collected rate data obtained in this study in which k_{obs} was calculated by using the integrated first-order rate equation. The solubility of H_2 in THF at 40.8 °C was taken[10] as 1.7×10^{-3} M atm^{-1}. The rate law (eq 1) for the hydrogenolysis of E is of the same form as that observed for alkene hydrogenation at a fixed H_2 pressure and suggests the reversible displacement of PPh_3 from rhodium by E followed by the rate-determining step which, in the present case, does not involve H_2.

Table III. Isotopic Exchange at Rhodium during the Reduction of 1-Phenylvinyl Acetate (E) (0.25 M) with H_2 (9.9×10^{-4} M) Using PPh_3 (1.9×10^{-3} M) and I-*3*-d_1 (2.1×10^{-3} M) in THF at 40.8 °C

catalyst precursor (purity)	reactants	no. of $[Rh]_t$ turnovers	recovered catalyst precursor purity, %
I-*3*-d_1 (93%)	E/Ar (control)	(3.0)[a]	73% D
I-*3*-d_1	E/H_2	3.1	59%D
I-*3*-d_1	E/H_2	8.0	39% D
I (100%)	E/D_2	5.0	100% H

[a] Reaction time equivalent to that required for 3.0 turnovers in hydrogenolysis.

Deuterium Exchange of I-*3*-d_1 with E and Scrambling during the Reaction of E with Deuterium. While the integrity of the deuterium label in I-*3*-d_1 was demonstrated to be very high during the hydrogenolysis of D and the reversible formation of an adduct[7] capable of deuterium scrambling was not apparent during these reactions, this result need not apply to E hydrogenolysis with I-*3*-d_1. Consequently, I-*3*-d_1 and E were equilibrated in the absence of H_2 (argon atmosphere), and hydrogenolysis reactions were also carried out under identical conditions save for the presence of 1×10^{-3} M H_2. These results are presented in Table III along with the results of isotopically reversed experiments in which I was employed in the hydrogenolysis of E using 1×10^{-3} M D_2. A series of the latter type of experiments was carried out under identical conditions in order to explore the distribution of deuterium in E, styrene, acetic acid, and ethylbenzene as a function of reaction time. These results are presented in Table IV along with the deuterium balance parameter,[4,5] Δ. When all D_2 which enters the hydrogenolysis process is accounted for and correctly located in the reactant and products, one observes a calculated value of $\Delta = 1.00$. Erroneous deuterium analyses or extraneous modes of deuterium incorporation would produce proportionate deviations of Δ from unity. The data presented in Table IV each provide Δ values that are essentially equal to unity. The GC/MS methods employed in obtaining the required deuterium analyses are described in the Experimental Section. Examination of I recovered after 9.7 apparent deuteriolysis turnovers by ^{11}B FT NMR gave no suggestion of B–D incorporation, since no loss of apparent B–H coupling was observed.

The results presented in Table III prove that the hydride ligand present on the rhodium center of I does not undergo exchange with D_2 during deuteriolysis of E. In the several experiments carried out in this mode with apparent rhodium turnover numbers between 2.8 and 9.7, no I-*3*-d_1 was observed. On the other hand, the equilibration of E with I-*3*-d_1 in the absence of H_2 (4-h duration) resulted in the transfer of deuterium label to E. The two hydrogenolysis experiments with I-*3*-d_1 of successively longer duration, gave diminishing recovery of D label. Thus, it may be concluded that there is no direct or indirect exchange of the hydride ligand present in I with H_2 during E hydrogenolysis although there is exchange of this hydride ligand with the methylene hydrogen atoms present in E. The postulation of the reversible formation of **1b** is therefore advanced to account for these results (see Scheme V).

The data presented in Table IV demonstrate the extensive scrambling of deuterium with the methylene hydrogen atoms of E during reactions conducted with D_2. Furthermore, the styrene product is reduced to ethylbenzene as a minor secondary product. Both the styrene and ethylbenzene are also formed with deuterium

(8) Long, J. A.; Marder, T. B.; Behnken, P. E.; Hawthorne, M. F. *J. Am. Chem. Soc.* **1984**, *106*, 2879.

(9) King, R. E. *Experimental Organometallic Chemistry: A Practicum in Synthesis and Characterization*; Wayda, A. L., Darensbourg, M. Y., Eds.; American Chemical Society: Washington, DC, 1987; Chapter 4.

(10) The authors are indebted to Professor Brian R. James and his coworkers for these solubility data.

Table IV. Isotopic Analyses of Products Resulting from the Reduction of 0.25 M 1-Phenylvinyl Acetate (E) with D_2 (9.8×10^{-4} M) Using I (2.16×10^{-2} M) and Triphenylphosphine (1.9×10^{-3} M) at 40.8 °C in THF

% rxn	turnovers, total Rh[a]	E anal., %			acetic acid anal., %		styrene anal., %					ethylbenzene anal., %						Δ[b]
		d_0	d_1	d_2	d_0	d_1	% prod	d_0	d_1	d_2	d_3	% prod	d_0	d_1	d_2	d_3	d_4	
21.3	2.80	93	7	0	0	100	21	36	52	11	1	0			N/A			1.01
37.0	4.35	88	12	0.5	0	100	36	43	43	14	0	1	0	18	51	31	0	0.95
74.4	8.78	79	20	0.5	0	100	68	35	44	20	2	6	2	20	44	26	7	0.96
83.1	9.72	68	30	2	0	100	73	27	46	21	6	10	2	21	47	25	4	1.00

[a] 100% reaction corresponds to 11.6 turnovers. [b] Deuterium balance calculated by using $\Delta = (\sum_{n=2}^{n=2} n[E\text{-}d_n] + \sum_{n=1}^{n=4} n[\text{EtPh-}d_n] + \sum_{n=1}^{n=3} n[CH_2{=}CHPh\text{-}d_n] + n[\text{AcOH-}d_n])/(3[\text{EtPh}] + [CH_2{=}CHPh] + [\text{HOAc}])$.

Scheme IV

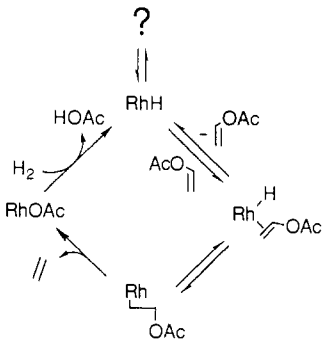

scrambling. It should be noted that while appreciable d_0-styrene is produced, the ethylbenzene is virtually free of d_0 species. *Most striking, however, is the fact that the acetic acid produced in these reactions is exclusively CH_3COOD.* Since the deuterium balance parameter, Δ, is nearly unity in all cases and since control experiments demonstrated no exchange between CH_3COOH and D_2 in the presence of I, it must be concluded that *the D atom of the CH_3COOD product is never involved in deuterium scrambling among the other organic components of the reaction and must be directly derived from D_2.* Consequently, acetic acid cannot arise from reductive elimination of a hydrido acetate in which the hydride ligand and alkenyl acetate reactant were simultaneously coordinated to the same Rh(III) center. This requirement limits the mechanistic possibilities for acetic acid formation in the catalytic cycle to a heterolytic dihydrogen cleavage by a rhodium(III) acetate accompanied by the appearance of a rhodium(III) monohydride. The rhodium(III) hydride then continues the catalytic cycle, as shown in Scheme IV, and serves as the obvious intermediate for the scrambling of deuterium into alkenyl acetate reactant. At this point, the question remains as to the detailed nature of the monohydride and the equilibria that describe its formation from I in accord with the overall rate law for the hydrogenolysis reaction (eq 1).

Proposed Mechanism for Alkenyl Acetate Hydrogenolysis. Scheme V presents the proposed mechanism for the catalytic hydrogenolysis of E with catalyst precursor I. This scheme is a simplified version of the situation that prevails since species such as **3** and **4** are mixtures of fluxional isomers and **5**, **6**, and related intermediates, which contain B–Rh σ bonds, exist in each case as a mixture of cage positional isomers. These complications are ignored in Scheme V and related schemes introduced later. Thus, as an example, all isomers of **6** are discussed as though they were a single generic species, **6**, etc. The monohydride alkenyl acetate complex **6** is in equilibrium with I, E, and triphenylphosphine (L) through a manifold of rhodium redox and ligand displacement reactions and the probable intermediates **1**, **3**, **4**, and **5**. Thus, the instantaneous concentration of **6** is given by the simple expression shown in eq 2. In the catalytic cycle which incorporates

$$[\mathbf{6}] = \frac{K[\mathrm{I}][\mathrm{E}]}{[\mathrm{PPh_3}]} \qquad (2)$$

6 as a reactant, the intermediate **9** is thought to repeatedly form and decompose reversibly (k_1 and k_{-1} steps) before the rate-determining β-elimination (k_2 process), leading to styrene and acetate **10**. Rapid conversion of **10** to **11** and thence to **6** may then proceed

Scheme V

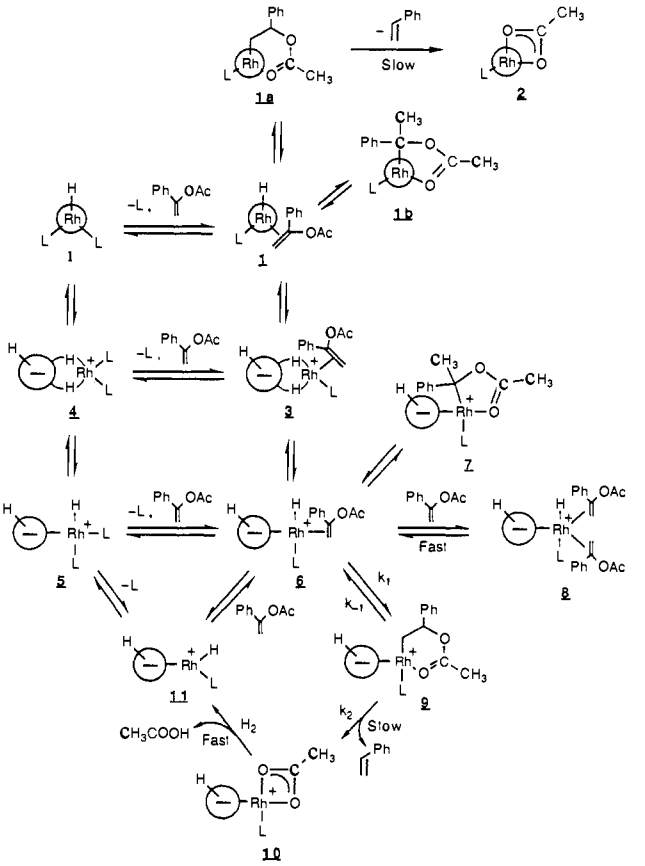

through a rapid heterolytic cleavage of dihydrogen. The rapid and reversible formation of **7** combined with the rapid exchange of E with **6** through the intermediate **8** (and perhaps via **11**) accounts for the scrambling of deuterium, when initially present on rhodium in **6**, into E and styrene product. The heterolytic cleavage of D_2 during the catalytic deuteriolysis of E leads to the formation of CH_3COOD, as observed, and rhodium-deuterated **11**. If, as indicated in Scheme V, the decomposition of **9** (k_2 process) is rate-determining, then the rate of hydrogenolysis is given by eq 3, which is equivalent to the experimentally observed eq 1 with $k_h = Kk_1k_2/(k_{-1} + k_2)$ and $[\mathrm{I}] \cong [\mathrm{Rh}]_t$.

$$\frac{-\mathrm{d}[\mathrm{H_2}]}{\mathrm{d}t} = \frac{Kk_1k_2[\mathrm{I}][\mathrm{E}]}{(k_{-1} + k_2)[\mathrm{PPh_3}]} \qquad (3)$$

The intramolecular reaction of the hydridoalkenyl acetate complex **1**, which leads to **1b**, would account for the observed loss of deuterium from I-*3*-d_1 when the latter species is equilibrated with E. The alternative mode of alkenyl acetate insertion could produce **1a**, which, in turn, could conceivably β-eliminate to form styrene and *closo*-acetate **2**. The latter sequence was not observed under the experimental conditions employed with E. However, heating I with D at 40 °C results in an analogous slow reaction which produces **2** and propene.[7]

Perhaps the most intriguing feature of the proposed alkenyl acetate hydrogenolysis mechanism is the incorporation of a reversible Rh(I) oxidative addition step which forms the active

Scheme VI

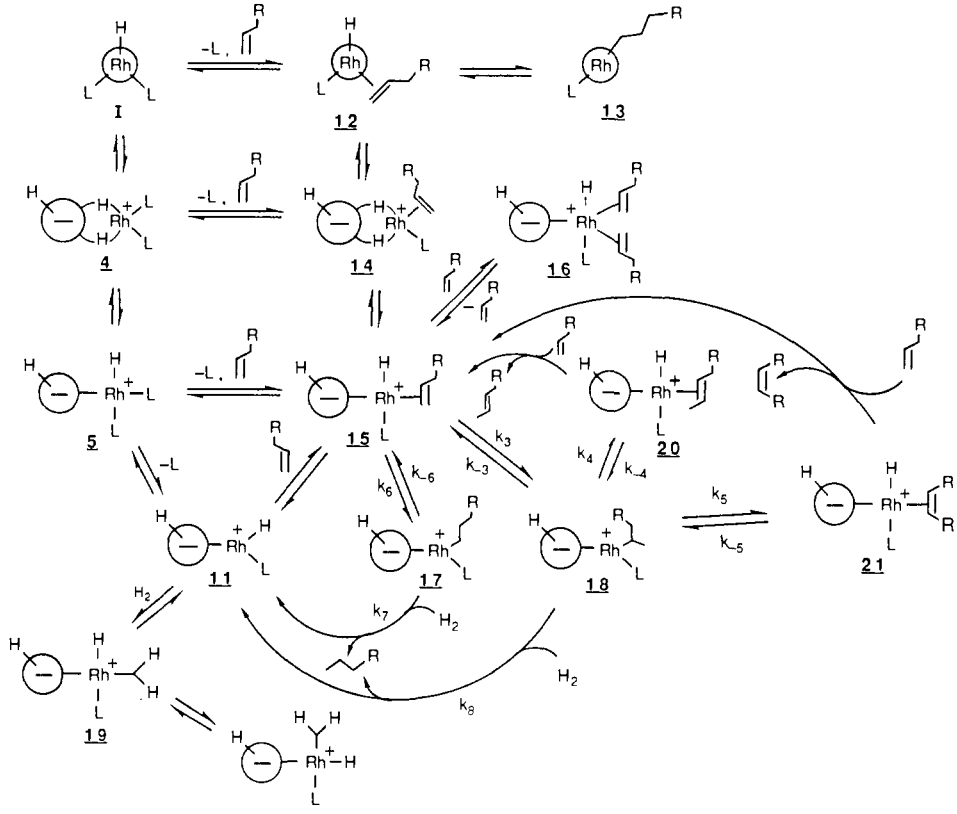

catalyst **6**. The direct reversion of **6** to *exo-nido*-**3** or its indirect reversion to **4** via **5** would perhaps be expected to result in the discernible incorporation of deuterium at the affected B–H vertices in reactions that employed D_2 and were carried through several equivalents of alkenyl acetate cleavage per mole of available rhodium. This expected transformation was not observed under the experimental conditions employed since no terminal B–D bonds could be detected using the loss of ^1H–^{11}B coupling in the ^{11}B FT NMR spectrum of recovered I as an experimental criterion. Clearly, the reactions that comprise the catalytic cycle proceed much more rapidly than the rate with which **6** is created from and returned to the pool of exo-nido and closo species which contains the preponderance of rhodium. Thus, as an example, if **6** is formed from and returned to the precursor pool at an arbitrary rate of 5 per unit time and if during that segment of time 100 hydrogenolysis cycles and associated ancillary cycles involving **7** and **8** occur, then one could not hope to detect deuterium exchange by only converting 10 or so moles of E to product per mole of rhodium present. Previously reported results[4] prove that the B(9,12) and B(10) vertices of I are those B–H groups that undergo facile exchange with D_2 and with 3-methyl-3-phenyl-1-butene-*1,1,2-d*$_3$. These same positions must represent the most reactive sites employed in the formation of the set of isomeric **6** species derived from I. The proposed structure of one possible isomer of **6** which is derived from the B(9) vertex of I is presented in Figure 2. The regioselective oxidative addition of Rh(I) to B–H bonds will be discussed fully in part II of this paper.

II. A Reinterpretation of Previous Results That Pertain to Alkene Isomerization and Hydrogenation

In paper 6 of this series,[4] the mechanisms of alkene isomerization and hydrogenation were explored with catalyst precursors I–III and [*exo-nido*-$(PPh_3)_2$Rh-μ-7,8-$(CH_2)_3$-7,8-$C_2B_9H_{10}$] (IV). Acrylate ester hydrogenation using catalyst precursors I and III was reported[5] in paper 7.

While the interpretation of the experimental evidence available at the time led to the mechanistic proposals presented in these two papers, it is now clear that those conclusions are, in part, incorrect.

In these previous reports,[4,5] the characteristics of the alkene isomerization and hydrogenation catalysts were recognized as clearly implicating a rhodium monohydride intermediate. Since this monohydride might have been formed by oxidative addition of the Rh(I) center present in *exo-nido*-rhodacarborane tautomers to B–H or C–H bonds, care was taken to evaluate these possibilities by deuterium tracer experiments. On the basis of these experiments, the intermediacy of a monohydride formed via intramolecular oxidative addition of Rh(I) to terminal B–H in exo-nido intermediates was rejected as a viable possibility since such processes as B–H exchange in I with deuterium during alkene reductions with D_2 were either very slow or absent under the conditions employed (no B–D detected in recovered I by NMR methods after 10 mol of reduction per mol of I charged). Also, the deuterium exchange actually observed between I-d_9, [*closo*-3,3-$(PPh_3)_2$-3-H-3,1,2-Rh$(CH)_2(BD)_9$], and 3-methyl-3-phenylbutene-1 (A) was similarly viewed as being too slow to provide a model for rapid alkene isomerization. These conclusions were based upon the related assumptions that each mole of alkane formed during alkene reduction with D_2 could be accompanied by the loss of a B–H bond and its replacement by B–D and that alkene isomerization must also involve a relatively rapid turnover of B–H bonds if B–Rh^{III}–H intermediates were present. As was shown above, these assumptions are misleading since a reactive B–Rh^{III}–H intermediate may very rapidly and reversibly form B–Rh^{III}–alkyl by reaction with alkene, but at the same time the B–Rh^{III}–H species itself may be formed and reversibly decomposed only relatively slowly in preliminary equilibria which contain closo and exo-nido precursors. This appears to be the correct analysis of the situation that prevails in virtually all of the known catalytic reactions of rhodacarboranes.

Results and Discussion

Kinetics and Mechanism of Alkene Isomerization and Hydrogenation. Scheme VI presents revised mechanistic suggestions for alkene isomerization and hydrogenation using any of the catalyst precursors I–IV. This proposal is based upon the slow and reversible formation of a set of monohydride cage positional isomers which, for purposes of simplification, are depicted as a single generic species, **15**. The generic **15**, which arises from closo

Scheme VII

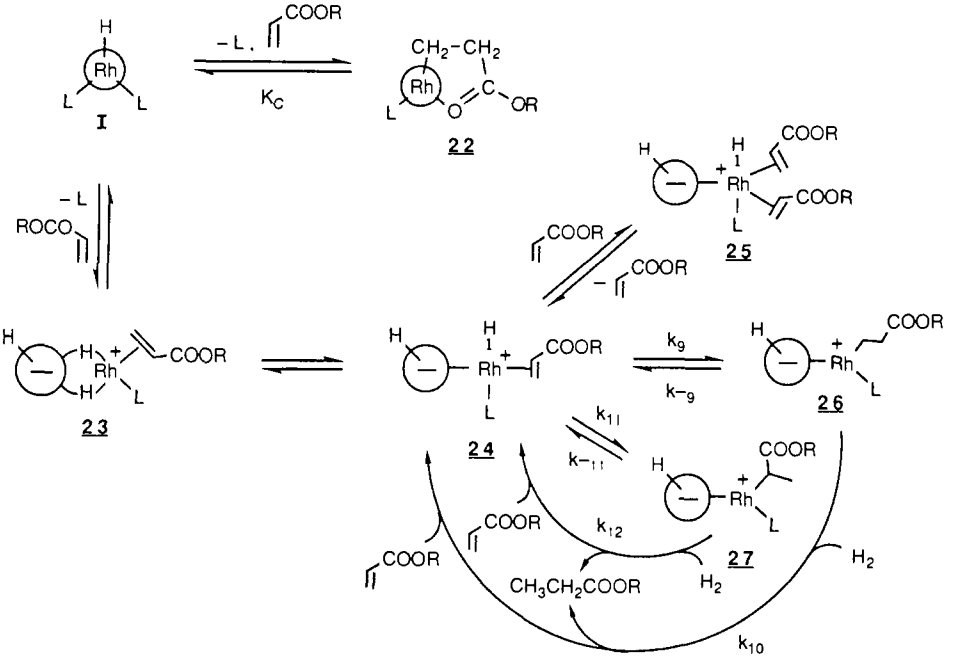

and exo-nido precursors as shown in Scheme VI, initiates a series of rapid reactions with alkene and hydrogen to provide the observed catalytic reactions. As in the case of alkenyl acetate hydrogenolysis, Scheme VI nicely satisfies the previously observed rate laws for 1-hexene (B) isomerization (eq 4) and the hydrogenation of A (eq 5). Again, the assumption is made that the

$$\frac{-\mathrm{d}[\text{1-alkene}]}{\mathrm{d}t} = \frac{k_i[\text{1-alkene}][\mathrm{Rh}]_t}{[\mathrm{PPh_3}]} \tag{4}$$

$$\frac{-\mathrm{d}[\mathrm{H_2}]}{\mathrm{d}t} = \frac{[\text{alkene}][\mathrm{Rh}]_t[\mathrm{H_2}]}{[\mathrm{PPh_3}](m + C[\mathrm{H_2}])} \tag{5}$$

steady-state concentration of the monohydride **15**, which is responsible for catalysis, is related to the rhodacarborane concentration (taken as being equal to $[\mathrm{Rh}]_t$), as well as the alkene and triphenylphosphine concentrations by the equilibrium expression (eq 6).

$$[\mathbf{15}] = \frac{K'[\text{alkene}][\mathrm{Rh}]_t}{[\mathrm{PPh_3}]} \tag{6}$$

In accord with Scheme VI, the rate of isomerization of a terminal alkene is given by eq 7, which recognizes independent pathways for the production of cis and trans isomers of 2-alkene (**18** → **20** → cis isomer and **18** → **21** → trans isomer). The rate constant k_i (eq 4) is thus defined as $K'[k_3(k_4 + k_5)/(k_{-3} + k_4 + k_5)]$ (eq 7). These cis–trans isomerization pathways appear

$$\frac{-\mathrm{d}[\text{1-alkene}]}{\mathrm{d}t} = \frac{K'[\text{1-alkene}][\mathrm{Rh}]_t}{[\mathrm{PPh_3}]}\left[\frac{k_3(k_4 + k_5)}{k_{-3} + k_4 + k_5}\right] \tag{7}$$

to be reversible using catalyst precursors I–III in 1-hexene isomerization since equilibrium mixtures of *cis*- and *trans*-2-hexene are observed. The nido precursor IV produces a preponderance of *cis*-2-hexene due to kinetic product control.

The experimentally determined rate expression for alkene hydrogenation is obtained from linear plots of k_h^{-1} versus $[\mathrm{H_2}]^{-1}$ where k_h is related to the observed rate of hydrogen consumption by eq 8 measured at constant $[\mathrm{H_2}]$. The observed slope, m, and

$$\frac{-\mathrm{d}[\mathrm{H_2}]}{\mathrm{d}t} = k_{obs}[\text{alkene}] = \frac{k_h[\text{alkene}][\mathrm{Rh}]_t}{[\mathrm{PPh_3}]} \tag{8}$$

intercept, C, of these plots are related to $[\mathrm{H_2}]$ by eq 9. From eq 5, the limiting rate of hydrogenation at infinite hydrogen pressure is $[\text{alkene}][\mathrm{Rh}]_t/[\mathrm{PPh_3}]C$. Consequently, $C^{-1} = K'(k_3 + k_6)$ from Scheme VI and m can be shown to equal $(k_{-3}k_6k_7 + k_{-6}k_3k_8)/$

$$\frac{1}{k_h} = \frac{m}{[\mathrm{H_2}]} + C \tag{9}$$

$k_3k_8k_6k_7K'$. Thus, the rate laws previously elucidated for A hydrogenation and B isomerization are easily reconciled with Scheme VI. Furthermore, the rate-limiting step required by the rate law in A hydrogenation at high $[\mathrm{H_2}]$ is clearly seen to be a set of parallel $(k_3 + k_6)$ steps, both of which result in $\mathrm{Rh^{III}}$–alkyl formation. Previously, this nuance of the hydrogenation rate law was given a quite different interpretation.

Mechanism of Acrylate Ester Hydrogenation. Scheme VII presents the proposed mechanism for acrylate ester hydrogenation using the catalyst precursor I or III but depicted with precursor I. As previously reported,[5] the species **22** (R = 1-butyl) is easily observed with $^{31}\mathrm{P}\{^1\mathrm{H}\}$ FT NMR, and its instantaneous concentration in kinetic experiments may be calculated from its formation constant, K_c. The concentration of **22** is identical with the simultaneous concentration of free $\mathrm{PPh_3}$, L. The resulting rate law for 1-butyl acrylate, C, hydrogenation with precursors I and III was previously derived[5] and shown to be identical in form with that observed in A hydrogenation[4] (eq 5, 8, and 9) after the instantaneous concentration of catalyst precursor I is corrected for the formation of **22** and the instantaneous concentration of $\mathrm{PPh_3}$, L, is set equal to [**22**]. As in the case of A hydrogenation, the instantaneous concentration of the monohydride **24** (as in the cases of **6** and **15**, here considered as a generic species) is given by eq 10 in which K'' is the equilibrium constant governing the

$$[\mathbf{24}] = \frac{K''[\mathrm{C}]\{[\mathrm{Rh}]_{tot} - [\mathbf{22}]\}}{[\mathrm{PPh_3}]} = \frac{K''[\mathrm{C}][\mathrm{I}]}{[\mathrm{PPh_3}]} \tag{10}$$

formation of **24** from I, C, and L. As previously suggested for A hydrogenation in Scheme VI, the formation and decomposition of the intermediate **23** is thought to be rapid, while the formation and decomposition of **24** is relatively slow. Thus, **24** may turn over many times in the hydrogenation cycle before it decomposes to **23** and reactants. The establishment of the equilibrium concentrations of **22** and $\mathrm{PPh_3}$ is also observed to be a slow process which results in the characteristic induction periods seen[5] in kinetic experiments.

As in the case of A hydrogenation,[4] Scheme VII may be reconciled with the experimental kinetic expressions, eq 5, 8, and 9, which also apply to C hydrogenation by equating C^{-1}, the limiting

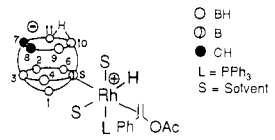

Figure 2. Proposed structure of one possible isomer of **6** derived from the B(9) vertex of *closo*-I, which is identical with the B(5) vertex in the nido numbering convention employed here. S represents solvent.

rate of hydrogenation at infinite hydrogen concentration, with $K''(k_9 + k_{11})$. The parameter m is given by $m = (k_{-9}k_{11}k_{12} + k_{-11}k_9k_{10})/k_9k_{10}k_{11}k_{12}K''$. Due to the complexity of the expressions that define the constants C and m in terms of reaction steps in Schemes VI and VII, it is impossible to make a meaningful numerical correlation of these terms when comparing the alkenes A and C or catalyst precursors I, III, and IV. Similarly, the precise definition of the small inverse deuterium kinetic isotope effects observed in A and C reduction ($k_{H_2}/k_{D_2} \cong 0.9$ in all cases investigated at 0.58 atm) is not possible.

Deuterium-Scrambling Reactions That Bear upon the Mechanism of Alkene Isomerization. It was earlier reported[4] that 1-hexene was rapidly isomerized by catalyst precursors I–IV in accord with the rate law described above and without exchange of deuterium attached to the Rh vertex in I-*3*-d_1. The latter observation provided the basis for the suggestion of closo–exo-nido equilibria[8] as a means of generating a reactive formal Rh^I center prior to alkene isomerization since the D atom would be retained in a B–D–B bridge bond of the exo-nido species and not available for reaction with alkene in an insertion reaction forming a *closo*-Rh–alkyl isomerization intermediate. Furthermore, it was amply demonstrated[4] that specifically deuterated propenes underwent rapid intermolecular D exchange both with themselves and with added alkenes such as A or 3,3-dimethyl-1-butene in the presence of precursor I. Again, it was shown that no loss of deuterium from I-*3*-d_1 took place during these reactions.

As a consequence of these results, it was thought possible that the observed catalysis was due to the presence of $B\text{–}Rh^{III}\text{–}H$ species produced by oxidative addition of L_2Rh^+ to a terminal B–H bond of *nido*-$C_2B_9H_{12}^-$ since both of these necessary reactants are present in the exo-nido isomers of I–III and in IV, which is itself an exo-nido species. In order to test this hypothesis, I-d_9, [*closo*-3,3-$(PPh_3)_2$-3-H-3,1,2-$Rh(CH)_2B_9D_9$], was prepared and employed in 1-hexene isomerization and in a deuterium-exchange reaction with A. As related in an earlier report,[4] no loss of B–D was observed by ^{11}B FT NMR line broadening (due to $^{11}B\text{–}^1H$ spin coupling) after 13 turnovers of I-d_9 in 1-hexene isomerization under kinetic conditions. Equilibration of I-d_9 and isotopically normal A in THF at 40.8 °C in near equimolar quantities and in the absence of added PPh_3 afforded the slow regiospecific exchange of the three alkenyl protons in A with the deuterium atoms attached to the B(9,12) and B(10) vertices of I-d_9. Since this observed exchange reaction was very much slower than 1-alkene isomerization reactions, the possibility was discounted that the $B\text{–}Rh^{II}\text{–}H$ intermediates demonstrated here (represented by **15** in Scheme VI) could be responsible for catalytic isomerization.[4]

The general Scheme VI for alkene isomerization and hydrogenation clearly predicts the eventual equilibration of alkene C–H with B–D vertices of the catalyst precursor as described above. The rate of this exchange process may remain quite low since, as repeatedly pointed out in this paper, the formation and decomposition of intermediates such as **15** may be a very slow process relative to all other reactions such as those involving prior closo–exo-nido equilibria and, of course, the catalytic cycle itself. In order to definitely prove that 1-hexene isomerization is accompanied by slow C–H/B–D exchange as demanded by Scheme VI, the isomerization of 1.95 M 1-hexene, with 3.25×10^{-3} M I-d_9 and 4.8×10^{-4} M PPh_3 was carried through 600 isomerization turnovers at 40.8 °C in THF solution. Recovery of the catalyst demonstrated clean exchange of the deuterium atoms present at the B(9,12) and B(10) vertices of the initial I-d_9. This result clearly demonstrates the validity of the $B\text{–}Rh^{III}\text{–}H$ intermediates depicted in Scheme VI and suggests that the several isomeric species depicted as generic **15** may live sufficiently long to turn over as many as 50–100 1-hexene molecules in isomerization to the isomeric 2-hexenes before reverting to their Rh^I exo-nido precursors. The previously reported[4] attempt to observe C–H/B–D exchange during as few as 13 turnovers must fail, as was the case.

Exchange of C–H with B–D in the earlier reported[4] very slow equilibration of I-d_9 with isotopically normal A is in agreement with the results of the 1-hexene isomerization/D-exchange reactions reported above since in both cases D exchange was cleanly observed at the B(9,12) and B(10) vertices of I-d_9. These are also the initial positions affected during the direct exchange of I with D_2 (vide infra).[4]

Deuterium Incorporation and Scrambling during the Reduction of A, B, and C with D_2 and Catalyst Precursor I. The manner in which D_2 was incorporated during the reduction of alkenes A, B, and C using I as the catalyst precursor[4,5] provides a further test of the validity of Schemes VI and VII. The reversible formation of rhodium alkyls such as **17** and **18** in Scheme VI or the corresponding **26** and **27** in Scheme VII when accompanied by the reversible formation of bis-alkene, **16**, and bis-acrylate ester, **25**, complexes requires deuterium to become distributed between alkene or acrylate ester reactant and the saturated reaction products. Furthermore, in the absence of rapid-exchange processes involving intermediates such as **19** in Scheme VI, which produce H–D exchange product, the total deuterium content of the system at any time should correspond to the moles of saturated product formed, and the previously defined D-balance parameter, Δ, should equal unity. Since the heterolytic cleavage of all rhodium alkyl intermediates with D_2 always introduces one D atom into the saturated products, one would not expect to observe the production of alkane-d_0 or propionate ester-d_0 in reactions that demonstrate a D-balance parameter of unity.

Catalyst precursor I was employed with alkenes A, B, and C and D_2 under kinetic conditions. The results of mass spectroscopic analyses of the reaction mixtures as a function of time were previously reported.[4]

Results obtained with alkene A (Table III, ref 4) clearly demonstrate the extensive scrambling of deuterium between alkene reactant and alkane product. The D-balance parameter, Δ, does not exceed unity throughout the experiment ($\Delta = 0.92 \pm 0.04$), and only trace quantities of 2-methyl-2-phenylbutane-d_0 are produced, as required by Scheme VI. During this experiment, it was observed that the RhH vertex of I retained its isotopic integrity, and a small amount of BH was exchanged for BD. The latter exchange could have occurred via collapse of **15** containing an exo-nido Rh^{III}–D center to form precursor I. Alternatively, the established slow direct exchange of D_2 with I,[4] discussed below, cannot be ruled out as the source of BD.

Reduction of 1-hexene, B, is difficult to accomplish with catalyst precursor I since B is rapidly isomerized to an inert, equilibrium mixture of 2-hexene isomers (Table VI, ref 4) which contains only 4–5% alkene-d_1. The very small quantity of alkane that is produced is, as expected, virtually pure hexane-d_1, and the recovered 1-hexene contains only a trace of deuterium. The D-balance parameter, Δ, was approximately 0.92 ± 0.04 but subject to some uncertainty, as were all analyses, due to the low conversions to deuterated products. Related to these observations is the fact that the ethylbenzene formed by reduction of the styrene product of E deuteriolysis is devoid of ethylbenzene-d_0 as presented in Table IV.

The reduction of 1-butylacrylate, C, with D_2 and catalyst precursor I was reported[5] to produce only trace amounts of 1-butyl propionate-d_0 and to proceed with scrambling of deuterium between C and product (Table II, ref 5). As before, the D-balance parameter, Δ, was near unity. It was apparent that D scrambling was less extensive in this acrylate ester system than with A, perhaps due to the fact that C is a more effective π-acceptor than A and the exchange of coordinated acrylate with bulk acrylate is relatively slower. The mechanisms depicted in Scheme VII appear to be in agreement with the presently known experimental facts.[5]

Mechanisms of Regioselective Exchange of D_2 with BH Vertices in Catalyst Precursors I and IV. As previously reported,[4] both

catalyst precursors I and IV undergo facile exchange of certain of their BH vertices with D_2 in THF solution at 40.8 °C. These reactions are inhibited by added PPh_3, and the exchange reactions observed with I are many times slower than those of IV, an exo-nido species. The RhH vertex of I does not undergo exchange during the course of B–H exchange with D_2. Due to the relatively slow exchange of I with D_2 under kinetic conditions, it was easily demonstrated that the B–H exchange sequence B(9,12) > B(10) > B(5,11) > B(6) ≫ B(8) ~ B(4,7) prevailed. Thus, as in the B–H exchange of I with A-d_3 and the B–D exchange of I-d_9 with isotopically normal B during isomerization, the B(9,12) and B(10) vertices of I selectively reacted with D_2. It should be noted that the more reactive B(9,12) and B(10) vertices in *closo*-I correspond to the B(5,6) and B(1) positions, respectively, in the exo-nido tautomer of I due to the different polyhedral numbering conventions that describe closo and nido cages.

While C–H/B–D exchange reactions have not been fully examined in the case of *exo-nido*-IV due to experimental complications, it has been possible to conduct a thorough study of B–H/D_2 exchange regioselectivity with this catalyst precursor. Unlike I, IV reacts very rapidly with D_2 (0.58 atm) in THF at 40.8 °C in the absence of added PPh_3, but the regioselectivity cannot be determined at this temperature. However, by reducing the temperature to 0 °C, it is possible to ascertain the relative reactivity of all the BH vertices by ^{11}B FT NMR spectroscopy with CO quenched reaction aliquots of IV obtained sequentially after definite time intervals. The CO quench formed $[(PPh_3)_2Rh(CO)_3]^+[nido\text{-}7,8\text{-}\mu\text{-}(CH_2)_3\text{-}7,8\text{-}C_2B_9H_{10}]^-$ in situ, in which the anion contained BD vertices. Two-dimensional ^{11}B–^{11}B FT NMR spectra confirmed the ^{11}B resonance assignments of $[nido\text{-}7,8\text{-}\mu\text{-}(CH_2)_3\text{-}7,8\text{-}C_2B_9H_{10}]^-$. The results of these experiments clearly demonstrated the decreasing reactivities: B(10) > B(9,11) > B(5,6) > B(2,4) > B(1) ≫ B(3). Vertex 3 could not be exchanged at room temperature after 48 h while B(10) was completely exchanged within 2 min at 0 °C. Vertices B(9,11) were fully exchanged after 4 min, and vertices B(5,6) were completely reacted within 30 min. For purposes of comparison, the exchange of vertices B(5,6) in I (numbered as nido tautomer) required ca. 1 h at 25 °C with D_2 (0.58 atm) and and in the absence of PPh_3, while vertex B(1) exchange was slightly slower under the same conditions.

The D_2 exchange reactions of I and IV, if comprised of generic intermediates such as **5**, **11**, and **19** of Scheme VI should, as observed, be inhibited by added PPh_3. The exchange process itself may be viewed as the coordination of D_2 to B–Rh^{III}–H as an electron pair donor ligand[11] followed by the restructuring of **19** through H- or D-atom motions in such a manner as to equilibrate H and D. This might be viewed as the heterolysis of D_2 by hydride **11** and would avoid invoking unattractive rhodium(V) trihydride intermediates.

Deferring to Scheme VI, it is clear that the dependence of D_2-exchange reactions upon intermediates such as **5**, **11**, and **19** allows the BH vertices that are exchanged to be identified as the same BH vertices attacked by Rh^I in forming **11** or its equivalent. Thus, the D_2 exchange results, when viewed as described below, provide a complete picture of the stereoelectronic effects which determine the preferred structures of the species denoted as **5** and **15** in Scheme VI when the steric encumberance of the $[nido\text{-}7,8\text{-}C_2B_9H_{12}]^-$ cage component is increased by substitution at both carbon atoms.

Figure 3 summarizes and compares the reactivities of the exo-nido tautomers of catalyst precursors I and IV (**4** in Scheme VI) with respect to competitive oxidative addition reactions of the Rh^IL_2 (L = PPh_3, alkene, or solvent) moiety with BH vertices and the B–H–B bonds characteristic of these particular exo-nido structures. Oxidative addition of the former type would produce a species depicted by **5** or **15** in Scheme VI, while reactions of the latter sort result in the formation of the corresponding closo tautomer. As in previous discussions of rhodacarborane reaction mechanisms, the two types of terminal BH hydrogen atoms, H_u and H_s, are distinguished in Figure 3 and Figure 4, which follow. The subscripts u and s refer to the placement of the H atom in

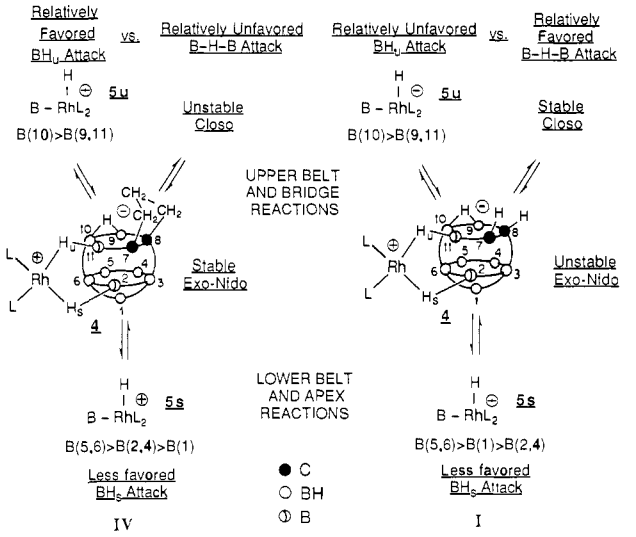

Figure 3. Pictorial comparison of the relative reactivities observed in the oxidative addition of terminal BH and bridging B–H–B bonds with cationic Rh^IL_2 derived from *closo*-I and its sterically encumbered counterpart, *exo-nido*-IV.

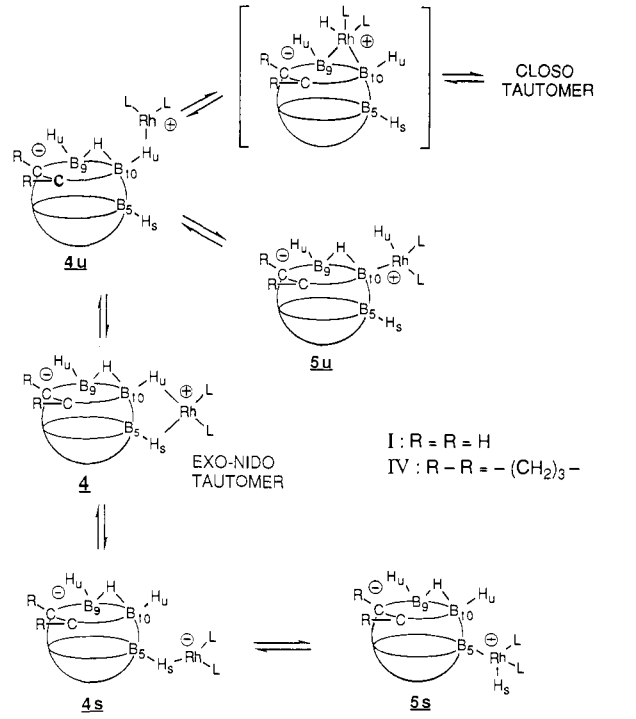

Figure 4. Simplified mechanistic descriptions of the contrasting behavior of *closo*-I and sterically encumbered *exo-nido*-IV depicted in Figure 3 and inherent in Scheme VI.

question upon an unsaturated B atom such as B(9,11) and B(10) or upon a saturated B atom such as B(5,6), B(2,4), and B(1), respectively, in the *nido*-C_2B_9 cage framework. Figure 3 indicates the relative stabilities of the closo and exo-nido tautomers of I and IV as well as the estimated relative importance of equilibria involving competitive oxidative addition reactions at BH_u and BH_s vertices and B–H–B arrays. The equilibria symbolized in Figure 3 are separated into two general categories. Reactions of the first category occur in the upper belt of BH_u vertices and the B–H–B bridge array. These equilibria are characterized by facile reactions that no doubt owe their rapidity to the presence of a unit of formal negative charge delocalized among the BH_u vertices of the *nido*-C_2B_9 cage and the accessibility of the associated bridging H atom in *exo-nido*-I. If attack by the positively charged Rh^IL_2 center is electrophilic in character, then enhanced reaction rates should prevail, as observed. The second category of equilibria

treated in Figure 3 is the attack of Rh^IL_2 upon BH_s vertices located in the lower belt and apical position of the *nido*-C_2B_9 cage. Oxidative addition of Rh^IL_2 to BH_s vertices does not proceed with the ease demonstrated in the similar BH_u reactions. This may be due to both the absence of a significant formal negative charge associated with the BH_s region of the *nido*-C_2B_9 cage and the presence of some steric repulsion of the bulky Rh^IL_2 center with the polyhedral surface in the BH_s region. It is quite clear, however, that the substitution of both carbon atoms of the nido cage, as in IV, profoundly affects the course of D_2-exchange reactions and, as discussed below, the selectivity of catalytic processes such as alkene isomerization and hydrogenation. These observations must relate to the differences in the stereochemical properties of the exo-nido tautomers of I and IV in the region of potentially more reactive BH_u vertices.

Figure 4 presents simplified mechanistic descriptions, derived from Scheme VI, that rationalize the difference in behavior of the catalyst precursors I and IV. To this end, it is instructive to consider the comparative behavior of the exo-nido tautomers of I and IV.

exo-nido-I (**4**) may generate the monobridged tautomer **4s** by rupture of the H_u–Rh^IL_2 bridge bond. **4s** produced in this manner may regenerate **4** or undergo oxidative addition of Rh^IL_2 to one of the designated B–H_s bonds, producing one **5s** (or **15s**) isomer which, in turn, enters the catalytic reactions of Scheme VI. If, on the other hand, an H_s–Rh^IL_2 bond is broken in **4**, one of the isomeric **4u** monobridged species is formed. The very reactive Rh^IL_2 center present in this species then makes a rapid and sterically unimpeded attack upon the B–H–B bridge array, thereby forming the very stable *closo*-I. Thus, the facile collapse of **4u** to *closo*-I essentially precludes the possibility of forming the terminal BH_u oxidative addition products such as **5u** when R = H. As a result of this stereochemical guidance, the catalytic chemistry resulting from I is only observed to occur with the use of BH_s vertices B(5,6) and B(1) in species such as **5s**.

The introduction of large organic substituents upon the carbon atoms of *closo*-I results in the steric destabilization of the closo tautomer, while the exo-nido tautomer **4** becomes relatively more stable. Thus, IV is isolated as the exo-nido tautomer **4**. The Rh^IL_2 centers present in the readily accessible isomeric **4u** derivatives of IV are therefore available either to undergo intramolecular oxidative addition to the B–H_u bond to which they are attached, thereby forming catalytically active species such as **5u**, or to return to **4**. As pointed out above, a reaction of this type, if electrophilic with respect to Rh^IL_2 attack, will be accelerated by attractive Coulombic forces available in the BH_u region of the *nido*-C_2B_9 cage. Collapse of **4u** to form unstable (and undetected) *closo*-IV is not an important competing reaction.

In summary, one may conclude that the catalytic reactions observed with the exo-nido tautomer of I occur at the BH_s vertices of the nido cage, B(5,6) and B(1), because vertices of the BH_u type are unable to compete with B–H–B for Rh^IL_2. However, due to stereochemical destabilization of the closo product of Rh^IL_2 attack upon B–H–B in the *exo-nido*-IV system, the catalytic reactions observed with this precursor predominantly occur at the electron-rich BH_u vertices of the nido cage, B(10) and B(9,11). Since these reactive BH_u vertices are near the carbon substituents in the catalytically active species, such as **5u** (or **15u**), the rates and selectivities of catalytic processes markedly differ depending upon the steric requirements about the *nido*-C_2B_9 cage carbon atoms. Observations of this sort have been previously reported[4] and are discussed below.

Hydrogenation of A Using Catalyst Precursor IV. The great rapidity with which precursor IV exchanges BH with D_2 may be explained bythe fact that, unlike precursor I, IV is an exo-nido species which does not require an unfavorable tautomerization from a closo structure in order to generate an Rh^IL_2 center suitable for oxidative addition to a terminal BH bond. Furthermore, the unique availability of the very reactive electron-rich BH_u vertices in the IV system further enhances the ease of **5u** or **15u** formation (see Figure 4). The enhanced reactivity of precursor IV is also demonstrated in the hydrogenation of A since the limiting rates, $C^{-1} = K'(k_3 + k_6)$, at infinite H_2 concentration are 3.4×10^{-6} s^{-1} for precursor I and 4.3×10^{-5} s^{-1} for precursor IV, respectively. This approximately 10-fold rate difference may reflect a more favorable equilibrium constant, K', for the formation of **15u** derived from *exo-nido*-IV than that of **15s** derived from *closo*-I.

The products of A reduction with D_2 and catalyst precursor IV were briefly examined and previously reported (Table V, ref 4). While the deuterium balance parameter, Δ, was near unity in these reactions, considerable scatter was observed. The appearance of a few percent of 2-methyl-2-phenylbutane-d_0 suggests that some exchange of D_2 with alkene CH is present in this system from **15u**-d_0 which produces HD via **11u**-d_0 and **19u**-d_2. Subsequent reaction of this HD with **17u** and **18u** species which are by happenstance free of deuterium (derived from **15u**-d_0) would form small amounts of alkane-d_0. These observations contrast with the results of A reduction using D_2 with catalyst precursor I (Table III, ref 4), discussed above, since only a trace of alkane-d_0 is observed in that case and alkane-d_1 is the dominant product. These results again demonstrate the enhanced reactivity of the catalytic species derived from precursor IV.

Competitive Hydrogenation and Isomerization of B Using Catalyst Precursor IV. It was previously demonstrated[4] that use of catalyst precursor IV allowed the hydrogenation (at 0.58 atm) of 1-hexene (B) to dominate by a factor of 11.5:1 the competitive isomerization of B to the hydrogenation-inert 2-hexenes. Separate B isomerization reactions using IV produced the isomeric 2-hexenes with a cis/trans of 5, while use of catalyst precursor I gave cis/trans of 0.5 under the same conditions. Obviously, the 2-hexene isomers produced with IV were formed under conditions of kinetic control. In control experiments, it was shown that the *cis*- and *trans*-2-hexenes were only very slowly interconverted with IV. Data were previously presented[4] which proved that B isomerization in the presence of IV was diverted to alkane formation by the addition of H_2 in such a manner as to suggest a common intermediate for both reactions. The proposed capture of **18u** (Scheme VI) by H_2 clearly predicts this behavior. The stability of the 2-hexenes produced by the decomposition of **18u** suggests that **20u** and **21u** are formed from **18u** in an irreversible manner and that the ratio k_5/k_4 determined the observed cis/trans of 5.

Reduction of B with D_2 using catalyst precursor IV was previously reported (Table VII, ref 4) and produced largely alkane and the expected 2-hexene isomer mixture in minor amounts. Interestingly, the deuterium balance parameter, Δ, was approximately 1.6 in these experiments, and large quantities of hexane-d_0 were observed along with deuterium exchange with B reactant. The isomeric 2-hexenes formed were of similar isotopic composition and far less deuterated at any time than B reactant. These data suggest that exchange of hexane-1 (B) with D_2 to produce HD and deuterated B is a facile reaction and that the HD produced may, in part, enter the final hydrogenation step and produce alkane-d_0. The dominance of reduction over alkene isomerization suggests that **17u** is readily formed and decomposed as shown in Scheme VI. On the other hand, **18u**, the 2-alkyl intermediate required for alkene isomerization, does not appear to play as important a role as does **17u**, and this must be due to steric encumberance of the 2-alkyl group with the μ-$(CH_2)_3$ substituents present on IV but absent in I and its exo-nido tautomer. Steric repulsions must also be responsible for the inability of the isomeric 2-hexenes to coordinate readily with the catalytic system provided by catalyst precursor IV and thereby undergo interconversions. While the general mechanisms for A hydrogenation and B isomerization described in Scheme VI appear to be generally applicable to *exo-nido*-IV in that the same rate laws are obtained with IV as with I and that other general reaction characteristics are comparable, the stereochemical requirements of IV are clearly much greater than are those of I as required by the mechanistic rationale presented in Figure 4.

Regiospecific Hydroboration of Catalyst Precursor IV with an Acrylate Ester Substrate. An investigation[12] of the reaction of

(11) For a recent discussion of H_2 as a ligand, see: Kubas, G. J. *Comments Inorg. Chem.* **1988**, *7*, 17.

Scheme VIII

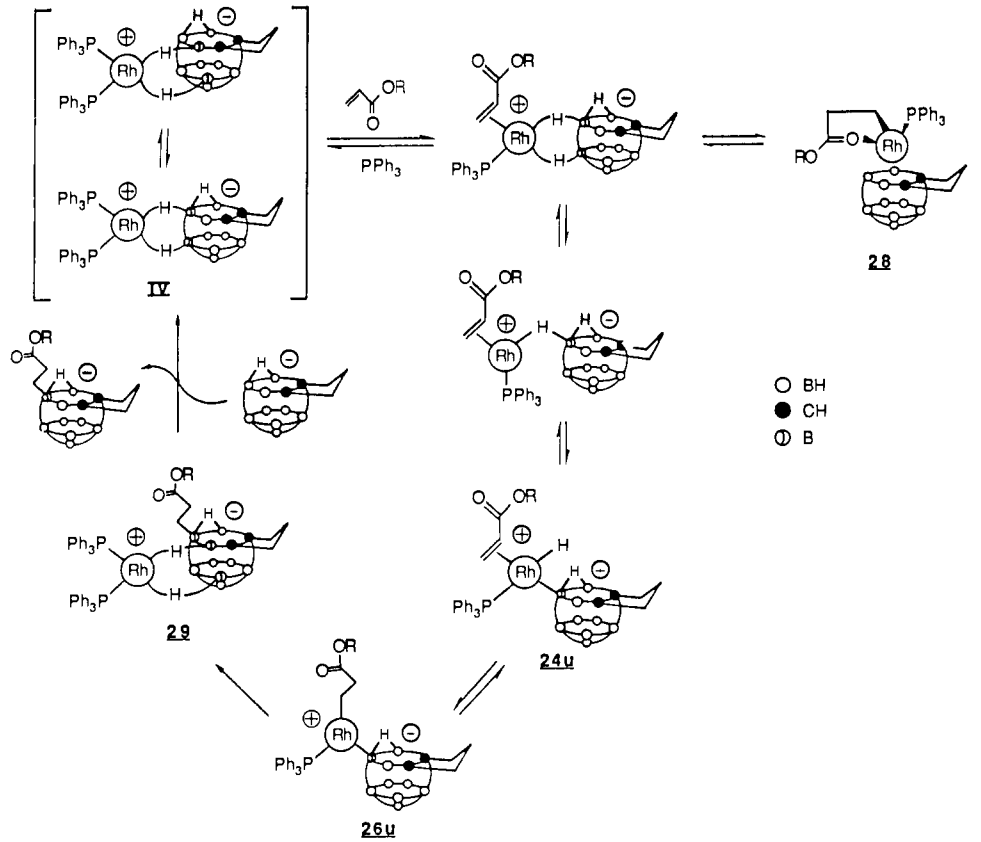

IV with 1-butyl acrylate in THF at 40 °C indicated the rapid and reversible formation of equal quantities of PPh_3 and a closo σ-bonded alkyl chelate formulated as **28** in Scheme VIII. After 5 days, the novel hydroboration product **29** was isolated in 69% yield and its structure determined[12] by an X-ray diffraction study. Products analogous to **29** could also be prepared with methyl acrylate or with *exo-nido*-rhodacarboranes [*exo-nido*-$(PPh_3)_2$Rh-7-R-8-R′-7,8-$C_2B_9H_{10}$] where R, R′ = CH_3, CH_3; CH_3, C_6H_5; and C_6H_5, C_6H_5. The B(10) vertex of each of these nido cages was the point of hydroboration as in the case of **29** derived from IV. Furthermore, hydroboration reactions of this sort were found to be specific for acrylate esters since no products could be identified in attempted reactions of IV with unactivated alkenes such as 1-hexene or other activated alkenes such as acrylonitrile and methyl methacrylate. Thus, the successful hydroboration of IV with alkyl acrylate esters is an unusual circumstance since these rhodium-promoted reactions are apparently quite sensitive to subtle stereoelectronic effects. It is important to note that only exo-nido C,C-disubstituted rhodacarboranes which have the BH_u vertex B(10) available for reaction with Rh^IL_2 are viable reactants. This may be due to the favorable equilibrium concentration of **24u** species (Scheme VII) formed with acrylate esters and the facility with which these intermediates insert acrylate to produce B_u–Rh^{III}–alkyl complexes (**26u**) capable of reductive elimination of B_u–alkyl and Rh^IL_2.

As shown in Scheme VIII, it was demonstrated that, by combining the hydroboration reaction of 1-butyl acrylate and IV with the rhodium-transfer reaction, which interconverts rhodacarboranes by anionic *nido*-C_2B_9 cage displacement,[13] it was possible to catalytically hydroborate 1-butyl acrylate at the B(10) vertex of the [*nido*-7,8-μ-$(CH_2)_3$-7,8-$C_2B_9H_{10}$]$^-$ ion. In this case, [*nido*-7,8-μ-$(CH_2)_3$-7,8-$C_2B_9H_{10}$]$^-$ displaces the hydroborated anion [*nido*-7,8-μ-$(CH_2)_3$-10-$(CH_2)_2$C(O)O$(CH_2)_3CH_3$-7,8-$C_2B_9H_9$]$^-$ from the hydroboration product regenerating IV.

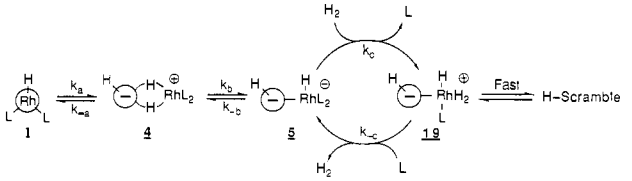

Figure 5. Simplified description of the two consecutive Rh redox equilibria which are responsible for the catalytic cycle based upon B–Rh^{III}–H catalysts.

No discussion of metal-promoted hydroboration is complete without recognizing the elegant work of Männig and Nöth[14a] in which a wide variety of alkenes, some of which bore functional groups, were cleanly hydroborated with 1,3,2-benzodioxaborole at low temperatures only in the presence of a catalytic quantity of $(PPh_3)_3$RhCl. These reactions clearly proceed via oxidative addition of B–H to $(PPh_3)_2$RhCl followed by alkene insertion into the resulting Rh–H bond and reductive elimination of the B–alkyl product. Oddly, rhodium catalysis with the $(PPh_3)_3$RhCl precursor was essentially limited to a single source of B–H; 1,3,2-benzodioxaborole. Evans et al.[14b] have extended this reaction and clearly demonstrated metal-directed hydroboration and its stereochemical consequences. The suggestion was made[14a] that the dioxaborole reactant was uniquely effective due to the relative acidity of the H atom attached to boron. In the rhodacarborane examples, it appears as though a positively charged and electrophilic Rh^IL_2 center preferentially attacks the most electron-rich BH vertex, B(10).

Concluding Remarks

Hopefully, the study reported here will serve to definitely establish the mechanisms of alkene isomerization, alkene hydro-

(12) Hewes, J. D.; Kreimendahl, C. W.; Marder, T. B.; Hawthorne, M. F. *J. Am. Chem. Soc.* **1984**, *106*, 5757.

(13) Long, J. A.; Marder, T. B.; Hawthorne, M. F. *J. Am. Chem. Soc.* **1984**, *106*, 3004.

(14) (a) Männig, D.; Nöth, H. *Angew. Chem., Int. Ed. Engl.* **1985**, *24*, 878. (b) Evans, D. A.; Fu, G. C.; Hovedya, A. H. *J. Am. Chem. Soc.* **1988**, *110*, 6917.

genation, and alkenyl carboxylate hydrogenolysis catalyzed by rhodacarboranes under mild conditions. The key to the proper description of these mechanisms lies in the recognition of three codependent but separate sets of equilibria represented in abridged form in Figure 5 (derived from Scheme VI) for the simple situation encountered in degenerate B–H exchange of a rhodacarborane with H_2. In Figure 5 and elsewhere in this paper, the assumption is made that the rhodacarborane exo-nido tautomer rather than the closo tautomer serves as the precursor to the catalytically active B–Rh^{III}–H σ-bonded complex. This assumption appears to be reasonable since the exo-nido tautomer contains Rh^{I} required for oxidative addition with the B–H σ bond. In addition, previously gathered structural information suggests that the exo-nido tautomer may convert to the B–Rh^{III}–H tautomer with a minimal change in molecular structure.

The relative rates of the k_a, k_{-a}; k_b, k_{-b}; and k_c, k_{-c} processes determine the characteristics of the catalytic reactions that have been investigated. In every case, the k_a, k_{-a} equilibria appear to be rapidly established[4,5] while reactions that form and decompose the B–Rh^{III}–H intermediate, k_b and k_{-b}, respectively, are apparently much slower than the reactions that comprise the true catalytic cycle (depicted as k_c and k_{-c}). Thus, the recognition of the ability of the relative long-lived B–Rh^{III}–H intermediates to support very rapid catalytic interconversions, independent of the possible reactions of the closo and exo-nido precursors with components of these catalytic reactions, constitutes the major new thrust of this study.

In work to be presented elsewhere,[15] it was observed that triethyl- or triethoxysilane could be employed with catalyst precursor I in the cleavage of alkenyl acetates, thus replacing H_2 as a reactant. Yields are quite good using this procedure, which may

$$CH_2{=}CHOCOCH_3 + HSiR_3 \rightarrow CH_2{=}CH_2 + R_3SiOCOCH_3$$

be carried out in a conventional Schlenk apparatus. The mechanism of these hydrosilanolysis reactions is under examination.

Lastly, it is appropriate to suggest that the McQuillin[16] hydrogenation catalyst derived from Py_3RhCl_3 and sodium borohydride in dimethylformamide solvent may owe its activity to the existence of a B–Rh^{III}–H species formed in situ. The degree of deuterium scrambling reported during the reduction of methyl 3-phenylbut-2-enoate with D_2 suggests the existence of an active rhodium monohydride catalyst center coupled with heterolytic cleavage of Rh–alkyl bonds in a manner analogous to that attributed to alkene hydrogenation with rhodacarborane precursors. The deuterated methyl phenylbutanoate product obtained under conditions typical for the use of the McQuillin catalyst gave analyses that correspond to 60% d_2, 33% d_1, and 6% d_3.

Experimental Section

General Comments. The 200.133-MHz ^1H and 81.02-MHz $^{31}P\{^1H\}$ NMR spectra were obtained by using a Bruker WP-200 Fourier transform spectrometer equipped with fixed-frequency probes, a deuterium lock, and a B-VT-1000 variable-temperature controller. The 126.93-MHz ^{11}B and $^{11}B\{^1H\}$ NMR spectra were obtained by using a Fourier transform spectrometer designed and built by Prof. F. A. L. Anet and co-workers (UCLA Department of Chemistry and Biochemistry). The one- and two-dimensional 160.45-MHz ^{11}B and ^{11}B–^{11}B spectra were obtained by using a Bruker WM-500 Fourier transform instrument equipped with a 64–202-MHz broad-band probe, a deuterium lock, and a B-VT-1000 temperature controller; the two-dimensional ^{11}B–^{11}B NMR were obtained on this instrument with a COSY routine using Bruker software on the Aspect 2000 computer.

The ^1H NMR spectra utilized tetramethylsilane (TMS) as an internal standard or used the residual proton resonances of the deuterated solvents (CH_2Cl_2, 5.34 ppm; C_6H_6, 7.2 ppm; $(CH_3)_2CO$, 2.04 ppm). The $^{31}P\{^1H\}$ NMR spectra utilized external aqueous 85% H_3PO_4 as a reference, with positive shifts taken as upfield resonances. The ^{11}B NMR spectra utilized external $BF_3{\cdot}(C_2H_5)_2O$ as a standard, with upfield shifts taken as positive.

Infrared spectra were obtained as Nujol mulls by using a Perkin-Elmer 317 or 710B spectrometer or a Beckman Model 1100 FT-IR spectrometer. Mass spectra were obtained at 70 eV using a Perkin-Elmer Sigma 3/Kratos MS 25 system equipped with a J & W Scientific, Inc., SE 52 glass capillary column. Routine GLC analyses were performed by using a Varian 1700 or Hewlett-Packard 5880 instrument using either 10% Carbowax 20M on acid-washed Chromosorb P column, a 27% $AgNO_3$/37% Carbowax 600 on Chromosorb P column, or a J & W DB-1 capillary column. Elemental analyses were obtained from either Schwartzkopf Microanalytical Laboratories, Woodside, NY, or Galbraith Laboratories, Inc., Knoxville, TN. Glovebox manipulations were conducted in argon-filled Vacuum Atmospheres AE-43 or AE-42-2 gloveboxes. Benzene and tetrahydrofuran were distilled from potassium metal, and ether was distilled from sodium–potassium alloy.

Materials. Benzene, tetrahydrofuran, diethyl ether (Mallinckrodt); isopropenyl acetate (Eastman); triphenylphosphine, 1-butyl acrylate (stabilized), *p*-methoxyphenol, sodium hydride (60% dispersion in mineral oil) (Alfa Products); argon, hydrogen (special purity 99.999%), deuterium (Liquid Carbonic); activity I alumina (Merck), and hydroquinone were commercially available. *closo*-3,3-$(PPh_3)_2$-3-H-3,1,2-$RhC_2B_9H_{11}$ (I),[6] I-d_9,[4] and I-3-*d*,[4] *closo*-2,2-$(PPh_3)_2$-2-H-2,1,7-$RhC_2B_9H_{11}$ (II),[6] *closo*-2,2-$(PPh_3)_2$-2-H-2,1,12-$RhC_2B_9H_{11}$ (III),[6] *exo-nido*-$(PPh_3)_2$Rh-μ-7,8-$(CH_2)_3$-7,8-$C_2B_9H_{10}$ (IV),[8] [*nido*-7,8-$C_2B_9H_{12}]^-$,[17] [*nido*-7,9-$C_2B_9H_{12}]^-$,[17] [*nido*-2,9-$C_2B_9H_{12}]^-$,[18] and [*nido*-μ-7,8-$(CH_2)_3$-7,8-$C_2B_9H_{10}]^-$[19] and 1-phenylvinyl acetate were prepared by literature methods. Acrylate esters and other alkenes were passed through activity I alumina, freeze-pump-thawed over CaH_2 three times and distilled in high vacuum immediately prior to use.

General Procedure for Kinetic Measurements of E Hydrogenolysis and Similar Experiments with D. All experiments were conducted in a constant pressure hydrogen titrator described previously.[4,9] THF was distilled from potassium under argon into a Schlenk flask. The solvent was then cannulated into an argon-flushed solvent reservoir, a 25-mL volumetric flask equipped with a rotoflow stopcock, and 12/30 standard taper through joint.

The reaction flask was loaded with the catalyst precursor and fitted with the solvent reservoir and the ice–water reflux condensor of the hydrogen titrator. After three cycles of evacuation and rifilling with argon, a PPh_3 solution in THF was added via syringe. (Where large quantities of PPh_3 were required, the PPh_3 was added as a solid with the catalyst precursor.) The THF was removed in vacuo, the flask was refilled with argon, and the rotoflow stopcock of the reservoir was opened to allow the solvent to enter the flask. The solution was stirred until the catalyst was dissolved. The system was then sealed and the solution frozen by passing a stream of liquid nitrogen between the reaction flask and the outer jacket. The gas remaining above the solution was removed by high-vacuum pumping, the system sealed, and the solution allowed to thaw. After three freeze–pump–thaw cycles, the system was refilled with hydrogen and the solid solution allowed to thaw. The reaction flask was fitted with hoses supplying water maintained at 40.8 °C from the constant-temperature bath and allowed to equilibrate under a hydrogen atmosphere along with vigorous stirring of the solution.

After the system reached thermal equilibrium, the stirring was stopped, the 1-phenylvinyl acetate (E) was injected by using an ultraprecision syringe, and the solution pressurized to the desired hydrogen pressure. The similarly pressurized mercury switch was opened to the reaction, the stirring resumed, and the timing counter reset. Collected rate data were treated using the integrated first-order equation and a locally written FORTRAN program.

Synthesis of Benzyl Magnesium Chloride of Low Toluene Content. All the necessary laboratory equipment for this synthesis was thoroughly dried (160 °C) and cooled in a dry environment or under vacuum. Magnesium turnings, 2.96 g (121.8 mmol), were placed in a 250-mL Schlenk flask. The flask was evacuated, and the magnesium was dried by heating it with a heat gun. After the flask was cooled, argon was admitted and 20 mL of dry degassed THF was syringed in. A small amount of benzyl chloride (2–3 mL) was added to initiate the reaction; then the remainder of the solvent (80 mL) and benzyl chloride (total amount: 14.8 g, 13.5 mL, 117 mmol) were added. The mixture was allowed to react a few hours, and the solution was cannulated away from the residual magnesium. The solvent was removed in vacuo, leaving behind a semicrystalline solid, which was washed with dry degassed heptane (3 × 40 mL) to remove most of the toluene. The solid was

(15) Kang, H. C.; Hawthorne, M. F., unpublished results.
(16) Abley, P.; Jardine, I.; McQuillin, F. J. *J. Chem. Soc., Chem. Commun.* **1971**, 840.
(17) Hawthorne, M. F.; Young, D. C.; Garrett, P. M.; Owen, D. A.; Schwerin, S. G.; Tebbe, F. N.; Wegner, P. A. *J. Am. Chem. Soc.* **1968**, *90*, 862.
(18) Busby, D. C.; Hawthorne, M. F. *Inorg. Chem.* **1982**, *21*, 4101.
(19) Paxson, T. E.; Kaloustian, M. K.; Tom, G. M.; Wiersema, R. J.; Hawthorne, M. F. *J. Am. Chem. Soc.* **1972**, *94*, 4882.

finally dried under vacuum and redissolved in dry degassed THF. The solution was found to contain ca. 2% free toluene relative to pure benzyl magnesium chloride.

Synthesis of CH_3COOD. In an argon-purged Schlenk tube, 2.6 mL of acetic anhydride was reacted with 0.5 mL of deuterium oxide, using 25 μL of acetic acid as catalyst. The mixture was stirred for 1 h at 40 °C, after which the solution became homogeneous. Analysis by ^1H NMR showed the product to be 96.3% CH_3COOD (by difference). This material was employed in a control reaction with toluene-free benzyl magnesium chloride for GC/MS calibration of the resulting toluene-d_1.

Control Reactions That Bear upon Deuterium Labeling. The following control experiments were performed to evaluate possible H–D exchange processes which could possibly interfere with deuterium labels introduced during E reduction with D_2.

A. Possible Conversion of Acetic Acid-d_0 to Acetic Acid-d_1 under Hydrogenolysis Conditions with D_2. One-hundred milligrams of I (0.13 mmol), 6.5 mg of triphenylphosphine (0.024 mmol), and 200 mg of acetic acid-d_0 (3.33 mmol) were equilibrated at 40.8 °C in the hydrogen titrator with 25 mL of THF and D_2 at 1 atm of total pressure for 16 h. The acetic acid was recovered by vacuum transfer of volatiles and transformed to toluene. GC/MS analysis proved this to be 100% toluene-d_0, i.e., the acetic acid was undeuterated. Consequently, no exchange occurs between AcOH and D_2 under catalytic hydrogenolysis conditions.

B. Possible Redistribution of D Labels by Equilibration of E Deuterolysis Products in the Presence of I. Four-hundred milligrams of I (0.52 mmol), 12.5 mg of triphenylphosphine (0.048 mmol), and 1.0 g of E (6.2 mmol) were dissolved in 25 mL of THF and reacted with D_2 (1 atm of total pressure) in the hydrogen titrator for 5 h. An aliquot was withdrawn and analyzed for the label distribution in the various products. The solution remaining in the reaction flask was freeze–pump–thawed three times to remove the deuterium. Argon was admitted to the system, and stirring was continued at 40.8 °C for ca. 15 h. The label distribution was analyzed again by GC/MS and showed no change from the first aliquot. Consequently, no deuterium was redistributed among the products of E deuterolysis.

Deuterium Distribution Resulting from E Reduction with D_2. The hydrogen titrator was employed in these experiments with D_2 and 1 atm of total pressure at 40.8 °C in THF solvent. The procedure was essentially the same as that described above for kinetic studies, except in the present case rate data were not collected, although the reactions were monitored by D_2 consumption. The results of these experiments are reported in Table IV. The procedure employed for product analysis at the conclusion of deuteriolysis follows: At the end of the reaction, an aliquot of the mixture (ca. 2 mL) was placed in an argon-purged Schlenk tube, which was then attached to an argon-purged transfer bridge. The system was freeze–pump–thawed twice, and the volatiles were vacuum distilled. The clear transferred solution was analyzed for its acetic acid content by gas chromatography (Carbowax 20M); only in this analysis are no special precautions taken to avoid H–D exchange due to moisture. The appropriate amount of stock benzyl magnesium chloride solution required to react with this acetic acid was then calculated. Under strictly moisture-free conditions, an excess (1.9 equiv) of this Grignand reagent was added to the acetic acid solution, and the mixture was stirred for 30 min at room temperature. Still keeping the system free from moisture, the volatiles were transferred under vacuum after two freeze–pump–thaw cycles. The volatiles were analyzed by gas chromatography to ensure that all the acetic acid had reacted to yield toluene. This solution was then analyzed by GC/MS for its toluene D-label content.

A second aliquot was used, after appropriate transfer of volatiles, to quantify each of the compounds in the final reaction mixture (gas chromatography, Carbowax 20M) as well as to determine their label content (GC/MS, DB5 column). The absolute quantities of each compound present were determined by correcting the obtained area percentages with the respective response factors.

Isotopic Exchange at Rhodium during the Reduction of E with D_2. Table III reports results of hydrogenolysis and deuterolysis of E under the usual conditions reported above for reactions in the hydrogen titrator. In each case, the volatiles were removed from the reaction mixture under high vacuum, and the solid residue was analyzed for Rh–D/Rh–H as previously described.[4]

Detection of BD/CH Exchange during the Isomerization of 1-Hexene (B) with I-d_{10}. In a typical reaction, a 100-mL Schlenk flask was charged with 5.0 mg (0.019 mmol) of triphenylphosphine and 100 mg (0.13 mmol) of I-d_{10}. Tetrahydrofuran (40 mL) and 6.4 g (78 mmol) of 1-hexene (B) were transferred to the reaction flask by trap-to-trap distillation under high vacuum. The resulting solution was equilibrated for 23 h (7 half-lives) in a 41 °C bath. The volatiles were then removed by vacuum. The residue of I was dissolved in a small volume of CH_2Cl_2 and passed through a short silica column to remove PPh_3. The CH_2Cl_2 solution of purified I was concentrated to 3 mL and added to 20 mL of pentane contained in a coarse glass frit funnel. The immediate precipitation of I resulted. The recovered solid was washed with pentane. The recovery of I was accomplished in 87% yield.

Gas chromatographic analysis of the volatiles determined the following composition: 1-hexene, 0.38%; *trans*-2-hexene, 19.63%; *cis*-2-hexene, 4.68%; THF, 75.31%, which signifies 600 catalytic turnovers, 98% isomerization of 1-hexene to 2-hexene, and a *trans*/*cis* 2-hexene ratio of 4.2:1. Column data: 40-m SE-54 capillary column; injector 100 °C, detector 200 °C, oven 40 °C for 5 min of ramping up to 140 °C at 10 °C/min. Retention times, in min: 1-hexene, 5.93; *trans*-2-hexene, 6.09; *cis*-2-hexene, 6.21; THF, 6.45.

FT IR spectra of recovered I in CH_2Cl_2 revealed enhanced absorption of the B–H stretch (2542 cm^{-1}) and decreased absorption of the B–D stretch (1923 cm^{-1}) due to H/D exchange at ~3.5 B atoms per cage. Similar exchange was observed at the Rh site (ν_{Rh-H} = 2084 cm^{-1}; ν_{Rh-D} = 1482 cm^{-1}).

The 164.4-MHz ^{11}B and $^{11}B\{^1H\}$ NMR spectra of recovered I were too broad to be informative. Conversion to the PEt_3 derivative provided sharp spectra, for which all signals have been assigned.[20] Comparison of ^{11}B spectra of PEt_3 derivatives of recovered and authentic I-d_{10} catalyst revealed substantial broadening and shortening of signals due to B(10) and B(9,12) and insignificant broadening of other signals in recovered catalyst.

Sequential Deuterium Exchange with IV, Producing IV-d_8. A 100-mL flask equipped with two rubber septum-sealed side-arm inlets with stopcocks was charged with IV (0.400 g, 0.5 mmol) and attached to an apparatus previously described.[4,9] Following an evacuation–argon-purge cycle, 35 mL of THF was added via a gas-tight syringe. A series of freeze–pump–thaw degas cycles was applied, the solution was thawed to 0 °C in an ice–water bath, and deuterium gas was vented into the flask. Deuterium gas was bubbled into the solution through a syringe needle inserted through one side arm (flow = 1 mL min^{-1}), and a timer was started. Aliquots of 3.0 mL were removed through the second side arm at intervals of 2, 4, 8, 30 min and 4 h; these were promptly injected into septum-equipped, CO-flushed 10-mL NMR tubes. The tubes were further purged of deuterium gas by either bubbling CO into the tubes or by two fast freeze–pump–thaw cycles. The samples containing partially B-deuterated $[(PPh_3)_2Rh(CO)_3]^+[nido\text{-}7,8\text{-}\mu\text{-}(CH_2)_3\text{-}7,8\text{-}C_2B_9H_{10}]^-$ were reduced in volume to ca. 2 mL and analyzed by using ^{11}B NMR spectroscopy. The assignment of BH vertices in the nido anion were made by ^{11}B–^{11}B two-dimensional FT NMR using a COSY routine as described above and elsewhere. Results are reported in the Results and Discussion sections.

The spectroscopic analysis of IV-d_8 (^1H and $^{31}P\{^1H\}$ NMR) were consistent with that of IV; the ^1H NMR spectrum of IV-d_8 (CD_2Cl_2) included a resonance at −2.6 ppm (br s, 1 H) due to a bridging B–H–B hydrogen atom. IR: 2676 (m) (residual B–H), 1923–1881 cm^{-1} (br m) (B–D).

Acknowledgment. The authors thank the National Science Foundation (Grant NSF-CHE-88-06179) for research support. Dr. David M. Schubert generously provided experimental assistance, and Andrea Owyeung produced the many illustrations.

(20) Kalb, W. C.; Kreimendahl, C. W.; Busby, D. C.; Hawthorne, M. F. *Inorg. Chem.* **1980**, *19*, 1590.